J|A|C|S ARTICLES

Published on Web 05/10/2010

Recognition of the Ring-Opened State of Proliferating Cell Nuclear Antigen by Replication Factor C Promotes Eukaryotic Clamp-Loading

John A. Tainer,[†] J. Andrew McCammon,[‡] and Ivaylo Ivanov*,[§]

Department of Molecular Biology, The Skaggs Institute for Chemical Biology, The Scripps Research Institute, 10550 North Torrey Pines Road, MB4, La Jolla, California 92037, Department of Chemistry and Biochemistry and Department of Pharmacology, Howard Hughes Medical Institute, Center for Theoretical Biological Physics, University of California, San Diego, 9500 Gilman Drive, La Jolla, California 92093-0365, and Department of Chemistry, Georgia State University, P.O. Box 4098, Atlanta, Georgia 30302-4098

Received January 14, 2010; E-mail: iivanov@gsu.edu

Abstract: Proliferating cell nuclear antigen (PCNA, sliding clamp) is a toroidal-shaped protein that encircles DNA and plays a pivotal role in DNA replication, modification and repair. To perform its vital functions, the clamp has to be opened and resealed at primer−template junctions by a clamp loader molecular machine, replication factor C (RFC). The mechanism of this process constitutes a significant piece in the puzzle of processive DNA replication. We show that upon clamp opening the RFC/PCNA complex undergoes a large conformational rearrangement, leading to the formation of an extended interface between the clamp and RFC. Binding of ring-open PCNA to all five RFC subunits transforms the free-energy landscape underlying the closed- to open state transition, trapping PCNA in an open conformation. Careful comparison of free-energy profiles for clamp opening in the presence and absence of RFC allowed us to substantiate the role of RFC in the initial stage of the clamp-loading cycle. RFC does not appreciably destabilize the closed state of PCNA. Instead, the function of the clamp loader is dependent on the selective stabilization of the open conformation of the clamp.

Introduction

Replication of chromosomal DNA is accomplished by a dynamic protein assembly termed the replisome.[1,2] Within the replisome, the function of replicative DNA polymerases (e.g., pol δ, pol ε)[3,4] is to rapidly and faithfully duplicate the cell's genetic material prior to cell division. Extension of the newly synthesized DNA strand occurs with extraordinary fidelity, progressing over thousands of nucleotides without interruption. During replication, proliferating cell nuclear antigen (PCNA)[5−7] serves as an accessory protein whose role is to topologically tether DNA polymerase to DNA. PCNA also acts as a scaffold in the recruitment of proteins involved in cell-cycle control and DNA repair.[8−12] Mounting recent experimental evidence has pointed to the involvement of sliding clamps in almost every aspect of DNA metabolism. Yet many mechanistic details of how these fascinating molecular adaptors are loaded onto DNA and function within the machinery of the replisome have remained enigmatic.

PCNA is composed of three equivalent subunits that come together to form a closed ring-shaped structure around DNA (Figure 1a). Since the link between PCNA and DNA is topological in nature, one-dimensional diffusion of the clamp along DNA (sliding) is uninhibited, while three-dimensional diffusion (coupled to dissociation) is suppressed. Thus, attachment to PCNA confers processivity to replicative polymerases by preventing premature dissociation from their DNA substrate. The fact that PCNA encircles DNA in a closed ring conformation necessitates an activated mechanism[13] for opening and loading sliding clamps onto primer−template DNA (i.e., a double-strand/single-strand junction with a 5′ overhang). In eukaryotic cells, this is accomplished by the action of a clamp loader assembly (Figure 1c), a multiprotein molecular machine that uses the energy of ATP binding and hydrolysis to open and reseal PCNA around DNA.[14] The clamp loading cycle (Figure 1b) involves initial association of PCNA with the

[†] The Scripps Research Institute.
[‡] University of California.
[§] Georgia State University.

(1) Benkovic, S. J.; Valentine, A. M.; Salinas, F. *Annu. Rev. Biochem.* **2001**, *70*, 181–208.
(2) O'Donnell, M. *J. Biol. Chem.* **2006**, *281*, 10653–10656.
(3) Johnson, A.; O'Donnell, M. *Annu. Rev. Biochem.* **2005**, *74*, 283–315.
(4) Burgers, P. M. J. *Chromosoma* **1998**, *107*, 218–227.
(5) Kelman, Z. *Oncogene* **1997**, *14*, 629–640.
(6) Krishna, T. S.; Kong, X. P.; Gary, S.; Burgers, P. M.; Kuriyan, J. *Cell* **1994**, *79*, 1233–1243.
(7) Moldovan, G. L.; Pfander, B.; Jentsch, S. *Cell* **2007**, *129*, 665–679.
(8) Dionne, I.; Nookala, R. K.; Jackson, S. P.; Doherty, A. J.; Bell, S. D. *Mol. Cell* **2003**, *11*, 275–282.
(9) Chapados, B. R.; Hosfield, D. J.; Han, S.; Qiu, J.; Yelent, B.; Shen, B.; Tainer, J. A. *Cell* **2004**, *116*, 39–50.
(10) Haracska, L.; Unk, I.; Prakash, L.; Prakash, S. *Proc. Natl. Acad. Sci. U.S.A.* **2006**, *103*, 6477–6482.
(11) Hoege, C.; Pfander, B.; Moldovan, G.-L.; Pyrowolakis, G.; Jentsch, S. *Nature* **2002**, *419*, 135–141.
(12) Maga, G.; Hubscher, U. *J. Cell Sci.* **2003**, *116*, 3051–60.
(13) Indiani, C.; O'Donnell, M. *Nat. Rev. Mol. Cell Biol.* **2006**, *7*, 751–761.
(14) O'Donnell, M.; Kuriyan, J. *Curr. Opin. Struct. Biol.* **2006**, *16*, 35–41.

 10.1021/ja100365x

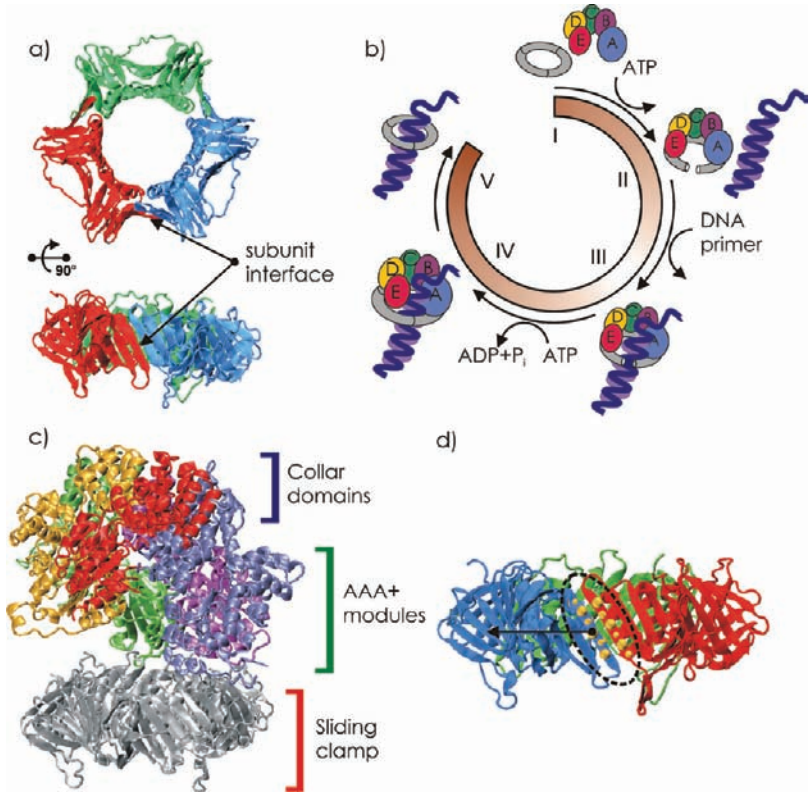

Figure 1. (a) Structure of the trimeric sliding clamp protein PCNA with the three equivalent subunits displayed in red, blue, and green, respectively; (b) schematic representation of the clamp loading cycle involving the action of the multisubunit clamp loader RFC. (c) structure of the yeast RFC/PCNA complex. We denote the five RFC subunits A−E according to their sequential order in the pentamer. Herein, we also provide an alternative nomenclature for the RFC subunits as follows: subunit Rfc1 (A), Rfc4 (B), Rfc3 (C), Rfc2 (D), and Rfc5 (E). The subunits A−E are colored in blue, purple, green, yellow, and red, respectively. PCNA is shown in gray. (d) Steered molecular dynamics applied to PCNA; the Cα atoms involved are shown explicitly (yellow spheres) and the in-plane pulling direction is indicated by an arrow.

pentameric replication factor C[15,16] belonging to the AAA+ family of ATPases[17] (AAA+ denotes ATPases Associated with various cellular Activities). ATP binding by the RFC subunits promotes disruption of one of the PCNA subunit interfaces. Threading of the nucleic acid through the resulting gap in PCNA and its subsequent interaction with RFC triggers ATP hydrolysis coupled to conformational changes in the RFC subunits. These changes, in turn, decrease the binding affinity of the RFC subunits for the outer surface of PCNA and lead to the eventual reclosing of the clamp around DNA and expulsion of the clamp loader.

Groundbreaking structural biology work has recently provided a first glimpse into the workings of the cellular machinery responsible for opening and loading sliding clamps onto DNA and delineated the common as well as divergent features of bacterial, archaeal, and eukaryotic clamp loaders.[13,16,18−20] This, in turn, resulted in the advancement of structure-based hypotheses regarding the function of these molecular machines. Specifically, in-plane versus out-of-plane models for clamp opening have been contrasted based on results from FRET[21] and EM (Electron Microscopy) experiments.[18] Molecular dynamics simulations revealed a natural tendency of the sliding clamp to flex in its open state into a right-handed spiral conformation and, thus, tentatively favored the out-of-plane model.[22] However, unified molecular-level understanding of the clamp loading process is currently lacking. Outstanding questions include: (i) what structural features of the clamp and the clamp loader are responsible for opening PCNA in the presence of ATP; (ii) does the sliding clamp remain planar as it opens or does it twist out-of-plane; (iii) is the gap between the PCNA subunits sufficient to accommodate dsDNA or is it only the ssDNA portion of the primer−template DNA that is threaded through the opening; (iv) what is the role of ATP binding and hydrolysis in the clamp loading cycle; (v) what is the nature of the conformational transitions responsible opening and for reclosing of the clamp around DNA?

The crystal structure of the *Saccharomyces cerevisiae* RFC/PCNA complex in the presence of a nonhydrolyzable ATP analogue (ATPγS) was solved by Bowman et al.[16] The structure shed light on the overall architecture of the clamp loader comprised of a rigid collar from which the nucleotide binding domains of RFC were suspended in a right-handed spiral arrangement (Figure 1c). Surprisingly, the structure revealed a closed conformation for the clamp, reminiscent of a late

(15) Bowman, G. D.; Goedken, E. R.; Kazmirski, S. L.; O'Donnell, M.; Kuriyan, J. *FEBS Lett.* **2005**, *579*, 863–867.
(16) Bowman, G. D.; O'Donnell, M.; Kuriyan, J. *Nature* **2004**, *429*, 724–730.
(17) Duderstadt, K. E.; Berger, J. M. *Crit. Rev. Biochem. Mol. Biol.* **2008**, *43*, 163–187.
(18) Miyata, T.; Suzuki, H.; Oyama, T.; Mayanagi, K.; Ishino, Y.; Morikawa, K. *Proc. Natl. Acad. Sci. U.S.A.* **2005**, *102*, 13795–13800.
(19) Dionne, I.; Brown, N. J.; Woodgate, R.; Bell, S. D. *Mol. Microbiol.* **2008**, *68*, 216–222.
(20) Seybert, A.; Singleton, M. R.; Cook, N.; Hall, D. R.; Wigley, D. B. *EMBO J.* **2006**, *25*, 2209–2218.
(21) Zhuang, Z. H.; Yoder, B. L.; Burgers, P. M. J.; Benkovic, S. J. *Proc. Natl. Acad. Sci. U.S.A.* **2006**, *103*, 2546–2551.
(22) Kazmirski, S. L.; Zhao, Y. X.; Bowman, G. D.; O'Donnell, M.; Kuriyan, J. *Proc. Natl. Acad. Sci. U.S.A.* **2005**, *102*, 13801–13806.

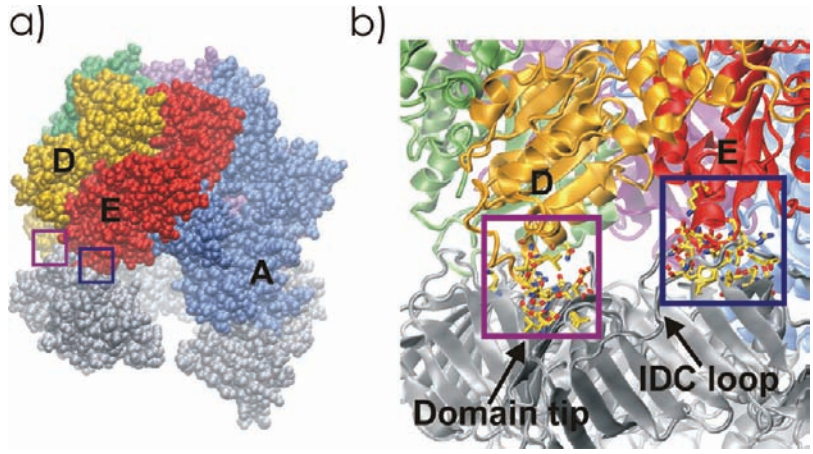

Figure 2. Computationally derived model for the complex of the clamp loader RFC with ring-open PCNA. (a) van der Waals surface representation of the model illustrates the out-of-plane twisting of the ring-open sliding clamp. Contacts with subunits D and E are highlighted by purple and blue rectangles. (b) Specific mode of interaction of the clamp with RFC subunits D and E.

intermediate in the clamp-loading cycle (state IV in Figure 1b). By contrast, EM imaging reconstruction[18] of an archaeal clamp loader/DNA/PCNA assembly unambiguously identified an open state of the sliding clamp bound to RFC (state II in Figure 1b). The conformation adopted by RFC in the X-ray structure had a helical pitch roughly matching the one of duplex DNA. Interestingly, the out-of-plane twisting of an open clamp, suggested by simulation, would also result in a right-handed helical conformation and the possibility of extending the binding interface between the clamp and the clamp loader. Thus, it is conceivable that RFC, rather than actively triggering the opening of PCNA, plays instead a more passive role in the initial step of the clamp loading cycle: to trap and stabilize the open conformation of PCNA. Herein, we set out to examine this hypothesis by computational means. A combination of steered molecular dynamics[23] (SMD) and the novel adaptive biasing force (ABF) method[24] were applied to establish favorable pathways and a thermodynamic framework for the opening of an isolated *S. cerevisiae* PCNA as well as PCNA in complex with the clamp loader RFC.

Results and Discussion

Clamp Opening by Steered Molecular Dynamics. The outer surface of yeast PCNA is composed largely of β-sheets that impart structural integrity to the clamp. The PCNA subunit interface is composed of two antiparallel β-strands that form part of the outer shell of the clamp (Figure 1a). The presence of hydrogen bonds and a considerable buried hydrophobic surface area between the two β-strands implies that disruption of the subunit interface is an activated process. Activated rare events are generally not accessible to direct molecular dynamics simulation. To circumvent this difficulty and enforce separation of the β-strands, we relied on steered molecular dynamics[23] (details are provided as Supporting Information: SI methods section and Figure S1). Specifically, we selected the Cα atoms of six residues from the first beta strand and applied external forces to steer the center of mass of these atoms away from the corresponding Cα atoms on the second β-strand (Figure 1d). SMD was used to force open the PCNA subunit interface in the in-plane direction for two cases: (i) an isolated sliding clamp and (ii) a clamp in complex with the clamp loader. It is essential to emphasize that at no point during the SMD run or during subsequent equilibration runs did we apply external forces in the orthogonal direction. Therefore, any observed out-of-plane displacement of the β-strands occurs spontaneously under the simulation conditions. Since the SMD simulations for the yeast RFC/PCNA complex were carried out in a highly nonequilibrium pulling regime, the runs were followed up by extensive 45 ns restrained molecular dynamics equilibration. For the subsequent 32 ns, all restraints were removed and the system was allowed to evolve freely toward an equilibrium conformation.

Stable Open Conformation of the Sliding Clamp Bound to RFC. Surprisingly, the equilibration dynamics led to a stable open conformation for the clamp in the presence of the clamp loader. By contrast, an open PCNA clamp in the absence of RFC recloses within nanoseconds even after substantial equilibration in the open state (Figure S2 and supplementary mpeg movie). We quantified the structural differences between the open-ring PCNA/RFC assembly relative to the closed-ring conformation from the X-ray structure. Calculated Cα atom root-mean-square deviations (rmsd) of 10.54 ± 0.55 Å were measured for PCNA, 3.36 ± 0.09 Å for RFC, and 8.72 ± 0.22 Å for the complex. The considerable flexibility of the ring-open sliding clamp appeared to be largely responsible for the observed structural differences with the original conformation (individual subunit rmsd values for PCNA are listed in Table S1; Figure S3 depicts the domain displacement in subunits S2 and S3 of the open structure relative to the closed conformation of PCNA). The clamp loader also adapted its shape to accommodate PCNA binding, although to a lesser extent. Upon opening, the PCNA subunits moved upward to match the right handed spiral arrangement of the clamp loader subunits (Figure 2a). Two clusters of residues originating from loops found at the base of subunits D and E were found to form new contacts with PCNA. It is worth noting that only subunits A, B, and C bind to PCNA in the X-ray structure of Bowman et al. whereas subunits D and E are suspended above the surface of the clamp making no contacts at all. By contrast our computationally derived open-PCNA/RFC model implies that all five RFC subunits are simultaneously attached to the clamp. Figure 2b illustrates the observed mode of binding: the first group of residues (from subunit D of RFC) binds close to the tip of the PCNA subunit; the second group (from subunit E of RFC) contacts a patch on the PCNA surface just below the interdomain connector (IDC) loop.

(23) Israelewitz, B.; Baudry, J.; Gullingsrud, J.; Kosztin, D.; Schulten, K. *J. Mol. Graphics Modell.* **2001**, *19*, 13–25.
(24) Darve, E.; Wilson, M. A.; Pohorille, A. *Mol. Simul.* **2002**, *28*, 113–144.

Residue distance maps (for Cα atoms) and cross correlation maps representing the interactions between the RFC subunits D, E, and PCNA in the open-ring complex are presented in Figure S4. Corresponding maps for the closed ring conformation do not display any Cα−Cα contacts closer than 20 Å and are, therefore, not shown. Residues 87−95 from chain D of RFC and residues 119 (PCNA subunit A), 169−172, 183−190, 217−219 (PCNA subunit C) from PCNA constitute the first cluster. Residues 93−97, 171 from chain E of RFC and residues 37−38, 53−56, 84−87 132−134, 136−138 from PCNA (subunit C) constitute the second cluster. The two clusters of residues appear in corresponding blocks highlighted on the distance map. Thus, our results are consistent with a model, wherein all AAA+ modules of RFC engage the sliding clamp in the open state. Our findings are in substantial agreement with recent work of Yao et al.,[25] which examined the roles of individual RFC subunits in opening PCNA. The authors determined that Rfc2•3•4•5 and Rfc2•5 subassemblies were capable of opening and unloading PCNA from circular DNA plasmids, suggesting that binding to Rfc5 (subunit E) was obligatory whereas binding to Rfc1 (subunit A) was not required to open PCNA. The study also used surface plasmon resonance to clearly demonstrate interactions of both subunits D and E (Rfc2 and Rfc5) with PCNA. The estimated K_d values of (480 nM for Rfc2-PCNA and 50 μM for Rfc5-PCNA) were 10- and 1000-fold weaker, respectively, than the values previously reported for the full RFC/PCNA complex, indicating that the full affinity of RFC to PCNA arose from the binding of all RFC subunits.

PCNA Opens Out-of-Plane. Another intriguing aspect of the clamp opening process is whether the sliding clamp remains planar as it opens or whether it twists out-of-plane. In-plane versus out-of-plane models have been debated in the literature based on different lines of experimental evidence. The EM reconstruction of an archaeal RFC/PCNA/DNA complex certainly invoked an out-of-plane mechanism.[18] However, the observed ∼6 Å gap in the density map was not large enough to allow duplex DNA to be threaded through the open PCNA interface. Another key piece of experimental evidence came from fluorescence spectroscopy. In an elegant study, Zhuang et al. introduced a FRET pair across the clamp interface (PCNA residues F185 and K107) and monitored the changes in PCNA topology along the different steps of clamp loading.[21] Addition of either ATP or ATPγS increased the measured distance between the FRET donor and acceptor residues from ∼13 to ∼34 Å, indicating that ATP binding to RFC was responsible for stabilizing an open conformation of the clamp. The authors proposed an in-plane model for the initial opening, followed, potentially, by an out-of-plane displacement in analogy to the clamp loading mechanism put forward for bacteriophage T4. We note that a 34 Å distance in the context of an in-plane model would certainly be sufficient to accommodate double-stranded DNA.

Both the FRET distance (F185−K107) and the out-of-plane strand displacement could be readily monitored along our trajectories. Thus, it is advantageous to compare directly our simulation results to the above experiments. Figure 3a displays the evolution of the distance between the side chain nitrogen atom (NZ) of residue K107 and a side chain carbon atom (CZ) of residue Phe185. The corresponding average distance in our model for the ring-open PCNA/RFC complex was 39.28 ± 2.95 Å in very good agreement with the experimental value. The deviation of ∼5 Å could be easily attributed to the different size of the mutated/labeled residues in the experiments or to our particular choice of side chain atoms to measure the distance.

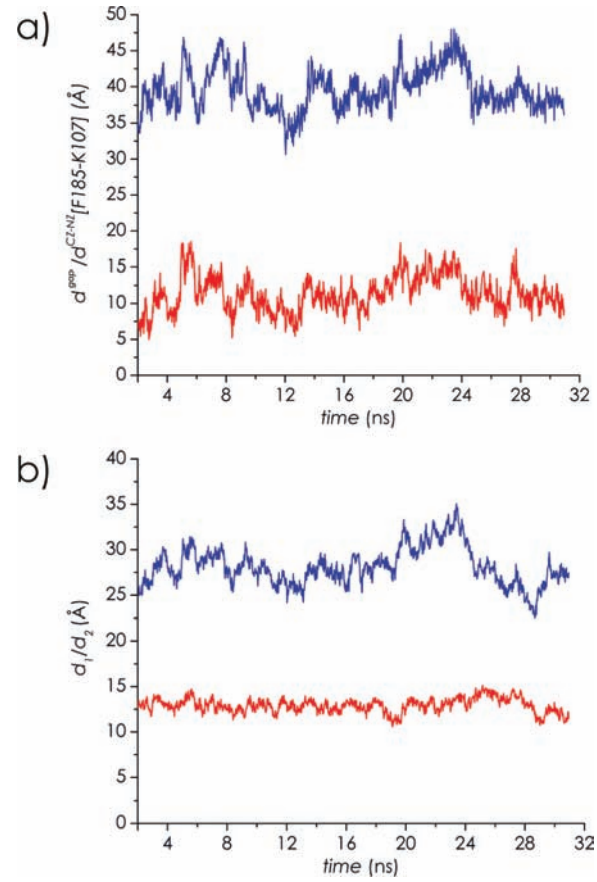

Figure 3. Time evolution of characteristic structural parameters. (a) The blue line corresponds to the distance (d^{CZ-NZ}) between the side chain nitrogen atom (NZ) of PCNA residue K107 and a side chain carbon atom (CZ) of PCNA residue Phe185 corresponding to the FRET donor−acceptor pair in the Zhuang et al. experiments. The red line represents the gap distance d^{gap} defined as the closest distance between heavy atoms from the two PCNA subunits across the open subunit interface. (b) The blue line displays the displacement between the centers of mass of all backbone atoms from the two interfacial β-strands projected into the plane of the PCNA ring (in-plane strand displacement). The red line displays the displacement between the centers of mass of all backbone atoms from the two interfacial β-strands projected along the normal direction to the plane of the PCNA ring (out-of-plane strand displacement).

Despite the apparent agreement in the extent of separation of the FRET residues in the open-state, we observed a marked shift toward a right-handed spiral PCNA conformation. Therefore, on the basis of our steered dynamics and subsequent equilibration, we favor an out-of-plane model for the PCNA opening transition and our open-state model (Figure 2a) closely resembles the EM reconstruction of RFC in complex with an open clamp.[18] We found that the average out-of-plane displacement (Figure 3b) of the two antiparallel β-strands during the last 32 ns of unrestrained molecular dynamics was 12.92 ± 0.79 Å. The value compares favorably to a recent simulation study (Kazmirski et al.)[22] wherein excursions from planarity of similar magnitude were noted for an open *S. cerevisiae* PCNA. However, as shown in Figure 3b, the clamp in complex with RFC maintained a stable out-of-plane twist throughout the simulation. By contrast, the simulations of Kazmirski et al. pointed to a frequent exchange between in-plane, right-handed

(25) Yao, N. Y.; Johnson, A.; Bowman, G. D.; Kuriyan, J.; O'Donnell, M. *J. Biol. Chem.* **2006**, *281*, 17528–17539.

and left-handed helical conformations, although the states with a right-handed helical twist were predominant.

The in-plane displacement of the β-strands forming the open PCNA interface (Figure 3b) was also monitored and displayed a larger range of variation between 22 and 34 Å. The average center of mass distance of the two β-strands was 28.14 ± 2.08 Å. The average gap distance in the subunit interface (Figure 3a) was 11.33 ± 2.45 Å. While the average gap in the open PCNA interface was marginally larger compared to the one observed in the EM map of Miyata et al.,[18] it was still too small to accommodate duplex DNA. Two scenarios could be put forward to explain how loading of primer−template DNA is accomplished. First, given the considerable flexibility displayed by ring-open PCNA in the simulations, the clamp may open wider when DNA is present. Indeed, the maximum gap distance of 18.6 Å observed in the simulations is just 5 Å below the lateral dimension of canonical B-form DNA. Second, it is possible that only the ssDNA portion of a DNA primer−template junction is threaded through the gap between the PCNA subunits.[18]

The Architecture and Electrostatics of RFC Favor Out-of-Plane Binding to Open PCNA. Several factors promote the out-of-plane opening of PCNA in the presence of RFC. First, the β-sheets forming the outer surface of the clamp possess an intrinsic tendency to flex toward a right-handed helical conformation, matching the spiral arrangement of the AAA+ modules in the ATP-bound form of the clamp loader. Second, the highly symmetric and modular architecture of the clamp loader is compatible with the pseudo six-fold symmetry of the clamp. This allows the RFC subunits to make extensive contacts at regular displacements along the surface of PCNA. Specifically, the subunits D and E present structural elements suitably positioned to attach to PCNA when the subunit interface of the clamp is disrupted. Finally, we note the significant electrostatic complementarity between the sliding clamp and the clamp loader. Figure 4 displays the electrostatic potential for PCNA and RFC mapped onto the molecular surface. The outer surface of the sliding clamp is highly negatively charged. By contrast, the interior of the clamp loader presents a surface of generally positive potential, suitable to accommodate primer−template DNA (Figure 4a). Additionally, we note the existence of a rim of positive charge not only on the inside, but also along the entire lower circumference of RFC (Figure 4b). The region of positive potential encompasses the locations where the AAA+ modules make contact with PCNA. Thus, in addition to structural factors, the out-of-plane motion of the ring-open sliding clamp appears to be guided by favorable electrostatics.

Free Energy of Clamp Opening in the Presence and Absence of the Clamp Loader. To gain deeper insight into the origin of stabilization of ring-open PCNA by replication factor C, we determined potentials of mean force (PMFs, effective free-energy profiles) along two reaction coordinates (ξ_1, ξ_2), representing approximate directions for clamp opening in the absence and presence of the clamp loader. The ξ_1 coordinate represents a distance along the in-plane opening direction. Likewise, ξ_2 represents a distance along the out-of-plane direction defined by the centers of the two interfacial β-strands in the ring-open model (detailed description of ξ_1, ξ_2 is provided as Supporting Information).

The potential of mean force for PCNA opening in the absence of RFC is shown in Figure 5a. Although the reaction coordinate ξ_1 was representative of the in-plane opening direction, out-of-plane twisting of the clamp was not restricted in any way. Its contribution is, therefore, included in the overall free-energy profile. Indeed, we note that out-of-plane displacement occurred

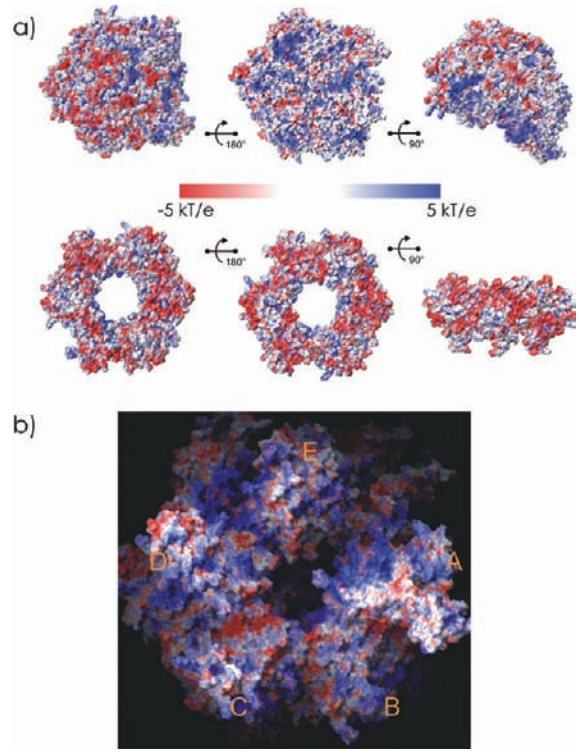

Figure 4. Electrostatic potential (ESP) mapped onto the molecular surface is shown for: (a) *S. cerevisiae* RFC and PCNA (anterior, posterior and lateral views are included for both proteins); (b) the internal cavity formed by the subunits of the clamp loader (labeled A−E) and the surfaces of the AAA+ modules responsible for binding to the sliding clamp. Regions of negative potential are shown in red; regions of positive potential are in blue.

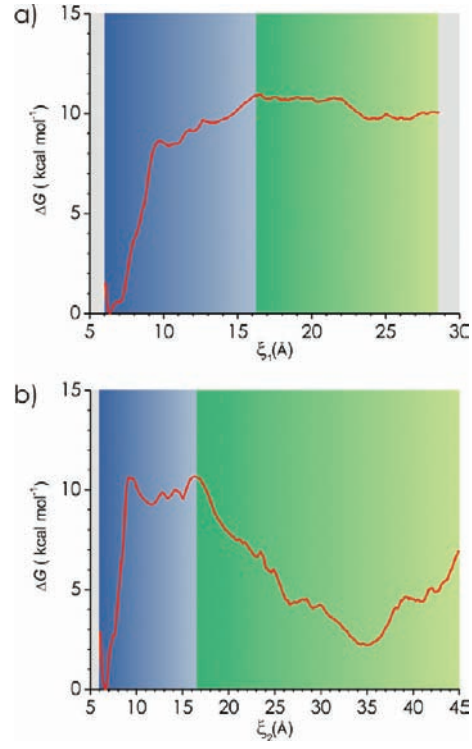

Figure 5. Potentials of mean force (PMFs) for PCNA opening. (a) PMF for in-plane opening of an isolated sliding clamp (in the absence of RFC); (b) PMF for opening a clamp bound to RFC.

spontaneously as we sampled windows with larger values of ξ_1, corresponding to open configurations.

The PMF profile revealed a seemingly uncomplicated picture for the PCNA opening transition in the absence of RFC. We observe three distinct regions. The first region, extending from ~6 to 10 Å, corresponds to the steep initial rise in ΔG as the system climbs out of the stable closed-state minimum. The abrupt rise signifies that disruption of the PCNA subunit interface is a highly cooperative transition (that involves unzipping of protein secondary structure elements). The second region (from ~10 to 17 Å) is characterized by a more moderate slope in the free energy landscape. After the last remaining subunit contacts have been broken, a broad plateau region follows, extending from ~17 to 29 Å. Within this region, the distance between the PCNA subunits could be extended with minimal energetic penalty. Thus, the PMF profile is consistent with the observed high flexibility of the ring-open PCNA in the free molecular dynamics runs. The overall free energy cost to open the sliding clamp is ~10−11 kcal/mol in agreement with experimental stability measurements.[26] We find no evidence for a "spring-loaded" opening mechanism as previously suggested for the *Escherichia coli* beta processivity clamp. A "spring-loaded" mechanism would imply the sliding clamp is inherently strained in its closed state. Consequently, disruption of the subunit interface should be accompanied by relaxation of the system into a stable open-ring conformation. The strain energy stored in the β-sheets forming the PCNA outer shell is expected to contribute to the barrier for the reverse process, the closing of the clamp. By contrast, we observe no appreciable stabilization anywhere beyond the initial free-energy minimum.

Another intriguing aspect of the above PMF is that the barrier to reclose the clamp is either minimal or essentially absent. Therefore, thermal fluctuation could drive the reclosing of the sliding clamp on a fast nanosecond time scale. This observation may explain how PCNA is able to fulfill its functions in the face of transient disruptions to the subunit interface occurring on a time scale commensurate with the time scale of replication (from milliseconds to seconds). It is worth noting that inevitable limitations in sampling may prevent inclusion of the full entropic contribution to the reverse free-energy barrier in the simulations. Despite this caveat, the qualitative result is clear: in the absence of other stabilizing interactions, a fast reclosing rate would kinetically prevent either ss- or ds-DNA from threading through the gap between the PCNA subunits. Furthermore, an elastic network model of an open PCNA clamp (Figure S5) indicates the direction of lowest energy mode is such that it would promote closing of the clamp. Thus, it is unlikely that transient disruption of the subunit interface would displace the clamp from DNA. Additional factors (such as the intrinsic affinity of DNA polymerase and the sliding clamp for DNA among others) undoubtedly contribute to the processive character of DNA replication. Therefore, the subunit interface stabilities are not the sole determinant of the clamp's ability to participate in processive replication and kinetic factors are also likely at play.

The potential of mean force for PCNA opening in complex with RFC is shown in Figure 5b and reveals a strikingly different picture of the clamp opening process when compared to profile for an isolated PCNA trimer (Figure 5a). First, we observe that the depth and shape of the initial free energy well (corresponding to the closed state of PCNA) is practically unchanged. Thus, it is reasonable to conclude that the action of the clamp loader does not involve significant destabilization of the closed conformation of the clamp. The barrier to disrupt the PCNA subunit interface is still ~11 kcal/mol. Once this barrier has been surmounted, instead of a plateau region, we observe a steady downward slope in the free-energy profile until a stable minimum is reached at a value of ξ_2 of ~35 Å. The depth of the free energy well induced by the binding of the clamp loader is ~9 kcal/mol. This value should, of course, be evaluated in the context of the accuracy of our ABF free-energy simulations, which is limited by a number of factors. Among those are: (i) the approximate nature of the chosen reaction coordinate; (ii) the difficulty of sampling all the orthogonal degrees of freedom in a system with 300 000 atoms; (iii) the accuracy of the force field; and (iv) the fact that the open state is represented by a computational model rather than an X-ray structure. Because of time scale limitations, it is conceivable that not all contacts between PCNA and RFC are fully optimal in our open state model. Thus, if a high resolution crystal structure had been available for the open state, the calculated stability of ring-open PCNA would have been even more substantial. Nevertheless, the qualitative picture of clamp opening in the presence of RFC is unambiguous: the open state of PCNA achieves comparable stability to the closed conformation within a difference of 1−2 kcal/mol. This difference is commensurate with the statistical inaccuracy of our sampling method for a system of this size and complexity.

We conclude that the role of the clamp loader in opening PCNA is to selectively stabilize the ring-open conformation. The association of the AAA+ modules of RFC with the outer surface of the open sliding clamp modifies the free-energy landscape underlying the closed- to open state transition and creates a stable free-energy minimum for the ring-open conformation of PCNA. In essence, residue contacts lost in the disruption of the PCNA subunit interface are compensated by newly formed contacts with RFC. These two interfaces appear to be mutually exclusive. In addition to thermodynamic stabilization of the open state, RFC binding increases the barrier for the reverse transition by ~9 kcal/mol. Decreasing the rate of reclosing ensures that the clamp remains open long enough to allow DNA to thread through the opening between the PCNA subunits.

Implications for the Biological Function of the Eukaryotic Clamp Loader. The presented effective free-energy profiles are instructive as they provide a lucid qualitative rationalization for the involvement of the clamp loader in the initial step of the eukaryotic clamp loading cycle. A schematic representation of our proposed model for the role of RFC in the clamp opening transition is presented in Figure 6. The key elements of the model are summarized as follows: (i) binding of ATP to RFC locks the clamp loader in a conformation that is both structurally and electrostatically compatible with the ring-open form of the clamp; (ii) following a transient disruption of the PCNA subunit interface, interactions with the AAA+ modules of RFC are optimized starting with subunit C and proceeding through subunits D and E; (iii) binding to RFC subunits subunits D and E is necessary to open PCNA; (iv) the association of PCNA with RFC results in an out-of-plane conformation of the PCNA ring within the assembly; (v) an interface complementary to ring-open PCNA transforms the free energy landscape underlying the closed- to open state transition, effectively trapping PCNA in an open conformation; (vi) the stability of the ring-open state in the presence of RFC is comparable to or greater

(26) Yao, N.; Turner, J.; Kelman, Z.; Stukenberg, P. T.; Dean, F.; Shechter, D.; Pan, Z. Q.; Hurwitz, J.; O'Donnell, M. *Genes Cells* **1996**, *1*, 101–113.

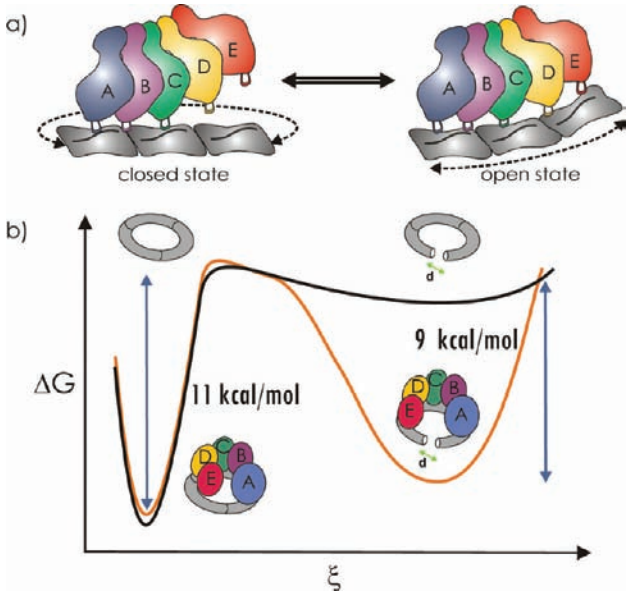

Figure 6. A proposed mechanism for the role of the clamp loader during the initial stage of the clamp loading cycle. (a) Schematic representation of the out-of-plane opening of PCNA upon binding of RFC and ATP. (b) Schematic representation of the change in the free energy landscape for clamp opening due to the complementary binding of RFC.

than the closed state; (vii) importantly, the open state is kinetically stabilized by a barrier for reclosing on the order of 9 kcal/mol.

To fulfill their varied functions at the replication fork, the sliding clamps have to strike a delicate balance between stability (high affinity for dimerization or trimerization) and the ability to open in order to be loaded onto primer−template DNA. There are two general strategies that could be exploited by the clamp loader to facilitate the opening of PCNA: energetic destabilization of the closed state or stabilization of the open state of the clamp. The two strategies are not mutually exclusive. Our analysis reveals that contrary to expectations,[27] RFC does not appreciably destabilize the closed state of PCNA. The function of the clamp loader is dependent rather on the selective stabilization of the open conformation of the clamp. The confluence of several structural and energetic factors enable preferential binding of RFC to the open-ring PCNA conformer: (i) the spiral arrangement of the RFC subunits; (ii) the intrinsic flexibility of the clamp and its tendency to twist out-of-plane; (iii) the favorable electrostatics; and (iv) the presence of structural elements of RFC poised to interact with PCNA. Comparison of free-energy profiles for clamp opening in the presence and absence of RFC implies that the contribution of the clamp loader to PCNA opening has both a thermodynamic and a kinetic component.

Materials and Methods

Model Construction. Models of the yeast PCNA clamp alone and in complex with the pentameric RFC clamp loader were constructed based on the available crystal structures (PDB accession code: 1PLQ and 1SXJ, respectively). Unresolved side chains in subunit A were modeled from the sequence using the program Modeler 8.[28] The nonhydrolyzable ATP analogue (ATPγS) was replaced by ATP at the RFC interfaces A−D. One ADP molecule occupied the D−E subunit interface. The models were completed by adding hydrogen atoms and solvated with TIP3P[29] water molecules using the XLeaP utility of AMBER 9.[30] Charge neutralization was accomplished by the addition of Na^+ and Cl^- ions. Excess salt concentration (~0.1 M) was introduced to mimic physiological conditions.

Simulation Details. The systems underwent a 2 ns equilibration in the canonical ensemble. The production runs were performed at ambient conditions in the NPT ensemble with the program NAMD 2.6[31,32] and the AMBER Parm99SB parameter set,[33,34] employing SPME electrostatics, 10 Å nonbonded short-range interaction cutoff, and the r-RESPA multiple time step method.[35] The simulations were carried out partly on the Abe machine at the National Center for Supercomputing Applications (NCSA) and primarily on the Jaguar machine at the Oak Ridge National Laboratory and required well in excess of half a million CPU hours (details are included in Supporting Information). SMD was used to force open the PCNA subunit interface in the in-plane direction for two cases: (i) an isolated sliding clamp and (ii) a clamp in complex with the clamp loader. The force constant k for the pulling runs was 6 kcal mol $^{-1}$ Å $^{-2}$ and the steering velocity υ was 3.0 Å/ns. For the RFC/PCNA system, SMD was followed by 45 ns restrained and 32 ns unrestrained molecular dynamics.

Adaptive Biasing Force Method. The adaptive biasing force method[24] as implemented in the NAMD2.6 package[32,31] by Chipot and Henin[36] was used to determine the effective free-energy profiles along the predefined intuitive coordinates ξ_1 and ξ_2 subdivided into a series of discrete windows. The sampling in each window varied from a minimum of 6 to 24 ns in order to ensure equilibration of the orthogonal degrees of freedom and even sampling along the reaction coordinates (details are provided as Supporting Information).

Acknowledgment. This research was funded by the Howard Hughes Medical Institute. Additional support was provided by the NSF Center for Theoretical Biological Physics at UCSD, National Biomedical Computational Resource and Accelrys, Inc. I.I. acknowledges support from Georgia State University through startup funds. Computer resources were provided by the National Center for Supercomputing Applications (NCSA) and by Oak Ridge National Laboratory through an INCITE allocation to I.I. at the National Center for Computational Sciences.

Supporting Information Available: Detailed methods section is provided describing model construction, steered molecular dynamics, the ABF method, and the electrostatic potential calculations. Supplementary references for the methods section are included. Additionally, five supplementary figures, one table and one molecular animation (in mpeg format) are included. This material is available free of charge via the Internet at http://pubs.acs.org.

JA100365X

(27) Barsky, D.; Venclovas, C. *Curr. Biol.* **2005**, *15*, R989–R992.
(28) Sali, A.; Blundell, T. L. *J. Mol. Biol.* **1993**, *234*, 779–815.
(29) Jorgensen, W. L.; Chandrasekhar, J.; Madura, J. D.; Impey, R. W.; Klein, M. L. *J. Chem. Phys.* **1983**, *79*, 926–935.
(30) Case, D. A. et al. *AMBER8*; University of California: San Francisco, CA, 2004.
(31) Phillips, J. C.; Braun, R.; Wang, W.; Gumbart, J.; Tajkhorshid, E.; Villa, E.; Chipot, C.; Skeel, R. D.; Kale, L.; Schulten, K. *J. Comput. Chem.* **2005**, *26*, 1781–1802.
(32) Kale, L.; Skeel, R.; Bhandarkar, M.; Brunner, R.; Gursoy, A.; Krawetz, N.; Phillips, J.; Shinozaki, A.; Varadarajan, K.; Schulten, K. *J. Comput. Phys.* **1999**, *151*, 283–312.
(33) Cornell, W. D.; Cieplak, P.; Bayly, C. I.; Gould, I. R.; Merz, K. M.; Ferguson, D. M.; Spellmeyer, D. C.; Fox, T.; Caldwell, J. W.; Kollman, P. A. *J. Am. Chem. Soc.* **1995**, *117*, 5179–5197.
(34) Duan, Y.; Wu, C.; Chowdhury, S.; Lee, M. C.; Xiong, G. M.; Zhang, W.; Yang, R.; Cieplak, P.; Luo, R.; Lee, T.; Caldwell, J.; Wang, J. M.; Kollman, P. *J. Comput. Chem.* **2003**, *24*, 1999–2012.
(35) Tuckerman, M.; Berne, B. J.; Martyna, G. J. *J. Chem. Phys.* **1992**, *97*, 1990–2001.
(36) Chipot, C.; Henin, J. *J. Chem. Phys.* **2005**, *123*, 244906.